Marine Pollution Bulletin 222 (2026) 118684

Contents lists available at ScienceDirect

Marine Pollution Bulletin

journal homepage: www.elsevier.com/locate/marpolbul

Shifts in microbial metabolism for algal-derived organic matter utilization under dynamic oxygen conditions

Quanrui Chen [a], Changjie Dong [a], Yuguo Li [b], Quan Shi [b], Xiaoxia Chen [a], Kai Tang [a,*], Nianzhi Jiao [a,*]

[a] State Key Laboratory of Marine Environmental Science, Innovation Research Center for Carbon Neutralization, Fujian Key Laboratory of Marine Carbon Sequestration, Xiamen University, Xiamen, 361102, PR China
[b] State Key Laboratory of Heavy Oil Processing, China University of Petroleum (Beijing), Beijing, 102249, PR China

ARTICLE INFO

Keywords:
Marine hypoxia
Heterotrophic bacteria
Algal-derived organic carbon
Organic carbon mineralization

ABSTRACT

The increase prevalence of hypoxic zones worldwide requires a comprehensive understanding of how marine organic carbon cycles under these conditions to assess their impact on global carbon cycles and ecosystem health. This study, conducted within the seasonal hypoxia zone of the Yangtze River Estuary, investigates the effects of deoxygenation on the microbial utilization of algal-derived organic carbon. Culture experiments and molecular analyses revealed remarkable adaptability in the composition and metabolic pathways of heterotrophic bacterial communities in response to hypoxic conditions. Findings demonstrate that while initial rates of dissolved organic carbon (DOC) utilization are reduced under hypoxia, the consumption over time is comparable to conditions of deoxygenation gradually. High-throughput 16S rDNA sequencing highlighted notable shifts in microbial community dynamics, with a consistent increase in the roles of key heterotrophic bacterial groups such as *Rhodobacteraceae*, *Flavobacteriaceae*, and *Vibrionaceae* in the transformation of organic carbon under reduced oxygen conditions. Importantly, hypoxia was found to induce more complex patterns observed in the transformations of dissolved organic sulfur. The depleted DOC molecules were predominantly composed of CHON and CHO. Under hypoxic conditions, unique microbial organic modules emerged, displaying positive correlations with dissolved organic sulfur (DOS) molecules, primarily involving the *Shewanellaceae* and *Bacteroidetes*. This research reveals specific microbial responses and metabolic mechanisms involved in the transformation of algal-derived organic carbon under hypoxic conditions. These findings improve our understanding of organic carbon cycling processes in hypoxic waters and offer new insights for future research on microbially driven carbon cycling.

1. Introduction

As human activities intensify, declining ocean oxygen has resulted in widespread hypoxia in coastal and open-ocean regions. Hypoxia is typically defined as dissolved oxygen (DO) concentrations below 63 μM (2 mg/L)(Diaz and Rosenberg, 2008).While biodiversity impacts have been well studied, the effects on marine organic carbon (OC) cycling remain poorly understood, underscoring the need to clarify OC–hypoxia interactions (Baroni et al., 2020; Diaz and Rosenberg, 2008). Estuarine and coastal regions, particularly influenced by nutrient inputs from rivers such as the Yangtze River Estuary, are experiencing significant expansion of hypoxic zones (Breitburg et al., 2018; Zhou et al., 2020; Zhu et al., 2017). The increase in hypoxic environments significantly impacts the metabolic capabilities of microorganisms in marine ecosystems, posing a considerable challenge to ecological balance (Engel et al., 2022; Jessen et al., 2017).

In oxic environments, aerobic microbial activity plays a pivotal role in the remineralization of OC (Yamuza-Magdaleno et al., 2024). However, under hypoxic conditions, the dynamics of this process undergo significant alterations. Consequently, the reduction in oxygen supply leads to shifts in microbial community composition and metabolic pathways (Bertagnolli and Stewart, 2018; Han et al., 2022). Seasonal hypoxia in coastal areas exhibits a coupled variation between apparent oxygen utilization and OC (Zhu et al., 2011). Primary production releases labile dissolved organic carbon (LDOC), which activates heterotrophic bacteria, enhancing the degradation of both new LDOC and pre-existing, more refractory OC– a process termed the marine priming effect (Guenet et al., 2010). The eutrophication of water column and the

* Corresponding authors.
E-mail addresses: tangkai@xmu.edu.cn (K. Tang), jiao@xmu.edu.cn (N. Jiao).

https://doi.org/10.1016/j.marpolbul.2025.118684
Received 26 January 2025; Received in revised form 6 September 2025; Accepted 6 September 2025
Available online 15 September 2025
0025-326X/© 2025 Elsevier Ltd. All rights are reserved, including those for text and data mining, AI training, and similar technologies.

mineralization of large amounts of OC by heterotrophic bacteria, has led to the deoxygenation of the water column, which has become a significant environmental issue (Dai et al., 2023). Generally, the reduced oxygen concentration in bottom waters leads to a greater accumulation of OC in marine sediments over a broad temporal scale (Katsev and Crowe, 2015; Keil, 1995). Following the onset of hypoxia, the microbial community shifts towards a predominance of facultative and obligate anaerobes. These microbes metabolize LDOC using alternative electron acceptors, such as nitrate or sulfate. Consequently, this shift in respiratory pathways constitutes a redox-driven form of the marine priming effect (Ragavan and Kumar, 2021). Additionally, in the presence of nutrients like ammonia, they produce extracellular enzymes capable of decomposing OC (Guenet et al., 2010). In addition, the emergence of fermentation processes, and these microbial metabolic activities allow the marine priming effect to persist even under hypoxia conditions.

In the seasonally hypoxic waters of the Yangtze River Estuary, hypoxia typically occurs at depths of 30–60 m in the bottom waters. Previous studies have identified surface algal blooms, primarily composed of diatoms, as the primary cause of oxygen depletion. These blooms contribute over two-thirds of the biogenic organic carbon in the estuary (Wang et al., 2017; Wang et al., 2016), leading to significant oxygen consumption in the water column, accounting for approximately 70 % of the apparent oxygen utilization (Zhou et al., 2021). Eutrophication in the estuary and hypoxic zones are also associated with high abundances of diatoms, including the representative genus *Thalassiosira,* which is widely distributed in global oceans and exhibits a high abundance in the Yangtze River Estuary (Li et al., 2018; Liu et al., 2024a; Malviya et al., 2016; Nelson et al., 1995). Previous studies have demonstrated that under deoxygenation conditions, the growth of *Thalassiosira pseudonana* may benefit from energy savings and reduced photoinhibition (Chen et al., 2021). Consequently, the accumulation of diatom-derived organic matter provides a critical oxygen-consuming pathway in seasonally hypoxic waters. Therefore, seasonal deoxygenation is closely linked to the rapid metabolic response of heterotrophic microorganisms to OC supply, generally occurring within days.

In the Yangtze River Estuary, frequent seasonal hypoxia has led to the adaptation of the local microbial community to fluctuations in redox conditions(Wang et al., 2016), making it an ideal area for studying heterotrophic bacterial populations capable of degrading diatom algal-derived dissolved organic matter (ADOM). Coastal habitats with algal-derived OC are dominated by *Flavobacteria*, which quickly respond to carbon inputs during remineralization (Teeling et al., 2016; West et al., 2008). The growth of these heterotrophic bacteria is intimately linked with the marine priming effect, directly influencing the mineralization of fresh OC (Williams et al., 2013). However, the impact of deoxygenation-anoxia conditions on the utilization of algal-derived OC by these heterotrophic bacteria remains unclear.

Based on prior observations of microbial resilience in seasonally hypoxic systems (Liu et al., 2024b), we hypothesize that microbial communities in the Yangtze River Estuary possess metabolic plasticity under oxygen-limited conditions. Specifically, while low DO may suppress short-term ADOM utilization, the long-term microbial carbon processing capacity will be maintained through community-level adaptation. This study, conducted in the seasonal hypoxia zone of the Yangtze River Estuary, aims to: (1) Evaluate the microbial utilization patterns of algal-derived OC under controlled deoxygenation-anoxia conditions in an incubation experiment; (2) assess the community and metabolic changes of heterotrophic bacteria in response to algal-derived OC under deoxygenation-anoxia conditions.; and (3) investigate how deoxygenation-anoxia affects the microbial processing of algal-derived OC. This study provides new insights into clarifying the limits of OC metabolism of marine heterotrophic bacteria and the transformation of OC utilization characteristics under hypoxia.

2. Methods

2.1. Acquisition of algal-derived dissolved organic matter (ADOM) and hypoxic water samples

ADOM was obtained from cultures of *Thalassiosira pseudonana* (CCMA.220), sourced from the Center for Collections of Marine Algae at Xiamen University, China. This genus has been previously identified in the water column of the Yangtze River Estuary and East China Sea (Jiang et al., 2015; Liu et al., 2024a). Sterilized surface seawater, collected near Xiamen, was enriched with F/2 with silicate medium (final concentration of 1 ‰) to cultivate *T. pseudonana* at 25 °C. Exponential phase cells were harvested using 0.7 μm GF/F filters (47 mm diameter, Whatman, UK) and subsequently lysed using an ultrasonic cell disruptor (SM-650D, Shunmatech, China) in an ice bath. The lysate was centrifuged (8000 rpm, 5 min, 4 °C) and further filtered through GF/F to obtain ADOM, which was then aliquoted and stored at −20 °C. All glassware was pre-burned at 450 °C for 6 h, and other materials were soaked in 2.5 % hydrochloric acid or acid-washed to remove potential OC contamination.

Bottom water samples were collected from stations A1 and A7, located in the Yangtze River Estuary (Fig. 1). Dissolved oxygen (DO) was measured *in situ* by CTD (Sea-Bird SBE 9, OxygenSensor SBE 43) data (A1: 31 m, 69.1 μmol/L; A7: 17 m, 100.1 μmol/L), in August 2021. The *in situ* hypoxic water was retrieved using shipboard CTD and immediately filtered through a 20 μm mesh and 3 μm polyester fiber membranes (47 mm diameter, Millipore, USA) to remove particulates while retaining microbial communities. The filtered seawater was transferred to acid-washed 20 L polyethylene buckets (PC, Nalgene, USA). For the hypoxic treatment groups, high-purity nitrogen was purged to establish low DO levels, whereas no nitrogen purging was applied to the oxygen-consuming and control groups. All seawater was then incubated in the dark at room temperature for 48 h to stabilize the *in situ* microbial communities.

2.2. Experimental design and sample collection

To investigate microbial utilization of ADOM under hypoxic conditions, we established three experimental groups for each station (A1 and A7 bottom water): (1) a hypoxic incubation group (DP), (2) an oxygen-consuming group (P), and (3) a control group (C, using bottom water from A1 only) that was maintained under *in situ* oxic conditions. Each group consisted of three replicates (Fig. 1). After initial settling, the filtered seawater was transferred into pre-combusted 2 L airtight glass bottles. For the DP group, dissolved oxygen was removed by sparging with high-purity nitrogen gas to establish hypoxic conditions (DO: 0–5 μmol/L), while the P and C groups were not artificially deoxygenated. After adding ADOM to the DP and P groups, the initial DOC concentration in the incubation bottles was approximately 1000 μM—about 8 times higher than the *in situ* DOC concentration. Nitrogen gas was used to maintain hypoxia in the DP group at each sampling point. DO concentrations in the incubation system were continuously monitored using in-bottle pre-attached oxygen sensor patches and optical oxygen meters (Sensor spots: SP-PSt7-YAU, PreSens, Germany) to ensure accurate DO levels. All culture bottles were kept for 7 days in a temperature-controlled (20 °C) dark incubator onboard.

Triplicate subsamples were withdrawn from each incubation bottle at both stations (A1 and A7) during the 7-day incubation. Nutrients, DOC and dissolved organic nitrogen (DON) were collected at 0, 0.5, 1, 2, 5 and 7 days; cell abundance at 0, 0.5, 1, 2, 3, 5 and 7 days, DOM optical spectra at 0, 1, 2 and 7 days; bacterial community composition at 0, 2 and 7 days; DOM molecular formulas at 0 and 7 days; and DOS concentrations at 0, 2 and 7 days. DOS was quantified as a diagnostic indicator of potential sulfur incorporation into DOM under hypoxic conditions. DOC and DON samples were filtered through pre-combusted GF/F glass fiber filters and transferred into 40 mL glass bottles, acidified

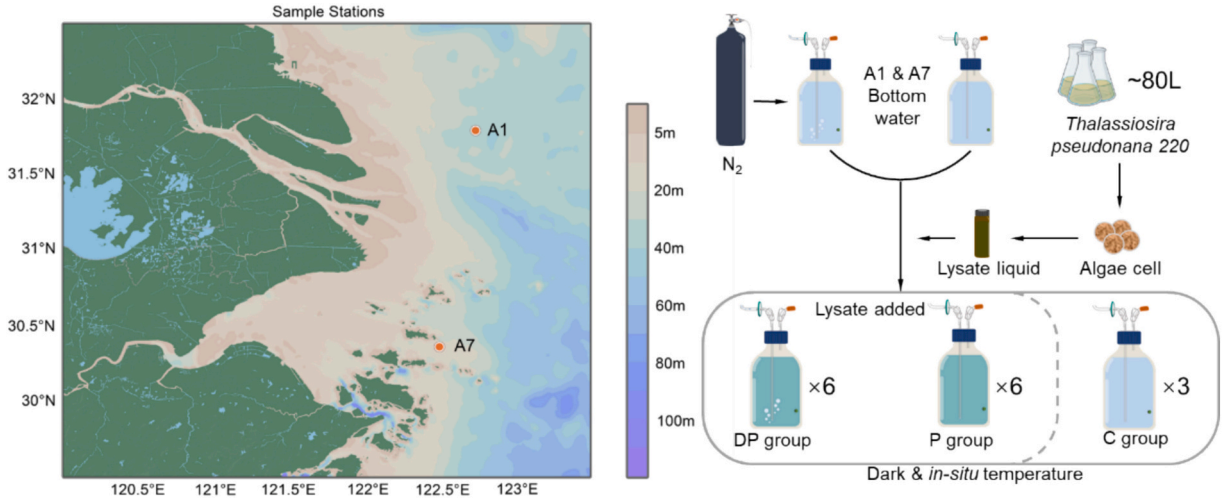


Fig. 1. Bottom water acquisition stations for culture experiment.

to pH = 2 with H_3PO_4. Microbial community composition samples were collected by filtering 500 mL of culture water through 0.2 μm pore size membranes (47 mm, Millipore, USA) pre-washed with Milli-Q water. Solid-phase extraction (SPE) was performed according to a previous study (Dittmar et al., 2008), using SPE columns (500 mg, Agilent Bond Elut PPL, USA) to extract DOM components and DOS concentration from the filtrate. All samples, except for microbial community molecular membranes (stored in liquid nitrogen), were preserved at −20 °C onboard.

2.3. Measurement of nutrients and cell abundance

Nutrient concentrations in the water samples were analyzed using a Technicon AA3 Auto-Analyzer (SEAL, Germany) for total nitrate and nitrite, silicate, and phosphate concentrations. Ammonium concentrations were determined using a modified orthophthaldialdehyde fluorometric method (Holmes et al., 1999). pH was measured using a PreSens optical microsensor (PM-HP5, PreSens GmbH, Germany) calibrated at 25 °C with pH 4, 7, and 10 buffers. Approximately 1 mL of nutrient-filtered residual sample was used for analysis.

Heterotrophic bacterial cell abundance in the culture system was measured using a BD Accuri C6 flow cytometer. Culture samples were thawed at 4 °C, and stained with 1 % SYBR Green I fluorescent dye (Invitrogen, Carlsbad, CA, USA) for 15 min in the dark before measurement. Samples with higher cell counts were diluted using Tris-EDTA (Sigma-Aldrich, pH 8.0, USA) after initial measurement to ensure accurate data acquisition (Marie et al., 1997). These parameters (DO, cell abundance, pH, nitrate, nitrite, and ammonium) are summarized in Supplementary Fig. S1 and were used to characterize the physico-chemical parameters during the cultivation period.

2.4. Determination of concentrations of organic carbon, nitrogen, and sulfur components

Concentrations of DOC and total dissolved nitrogen (TDN) were determined using the Shimadzu TOC-VCPH analyzer. DON concentration was then calculated by subtracting the concentration of inorganic nitrogen from TDN.

$$DON\ (\mu mol/L) = TDN - C(NO_3^-) - C(NO_2^-) - C(NH_4^+)$$

DOS concentrations were measured using Inductively Coupled Plasma Optical Emission Spectroscopy (ICP-OES, 5110vdV, Agilent Technologies, USA). The methodology followed Pohlabeln et al. (Pohlabeln et al., 2017), where enriched DOC was eluted into pre-burned sample bottles using 6 mL of methanol. From the eluate, 2 mL was transferred to pre-burned amber glass bottles for solid-phase extraction of DOC (DOC-SPE), while the remaining 4 mL was allocated for solid-phase extraction of dissolved organic sulfur (DOS-SPE) and subsequently dried under a nitrogen stream. The final DOC-SPE samples were redissolved in 30 mL of ultrapure water and analyzed for concentrations using a Shimadzu Total Organic Carbon Analyzer. DOS-SPE samples were redissolved in 10 mL of 5 % nitric acid for quantification *via* ICP-OES. DOS concentrations were estimated based on the recovery rates of DOC.

$$DOS\ (\mu mol/L) = (DOS - SPE^{*}\ DOC)/DOC - SPE$$

The extraction efficiency of the PPL column was represented by the ratio of DOC-SPE to DOC concentration. The concentration of DOS in seawater was obtained by dividing the DOS-SPE concentration by the extraction efficiency of the PPL column.

2.5. Measurement of fluorescence spectral information

To characterize the composition of DOM and identify potential changes under hypoxic conditions, fluorescence spectral information for the samples was measured at room temperature using a three-dimensional fluorescence spectrophotometer (Horiba Aqualog, Japan) to analyze the fluorescent dissolved organic matter (FDOM) in DOC. Blank corrections were performed with Milli-Q water. Samples were transferred to 1 cm path-length quartz cuvettes and scanned at a constant room temperature with an excitation duration of 2 s, covering an excitation wavelength range of 250–600 nm and an emission scan range of 250–800 nm, with a resolution of 2 nm to generate excitation-emission matrices. Three-dimensional fluorescence spectral data were processed using the R software package StaRdom (Pucher et al., 2019). Parallel Factor Analysis (PARAFAC) was employed to decompose the excitation-emission matrice spectra into multiple components, and comparisons were made with corresponding fluorescent groups reported in the OpenFluor database (http://www.openflor.org).

2.6. LC-Orbitrap MS analysis and measurement

To gain a more detailed understanding of the composition of DOM, eluted DOC-SPE was analyzed using an Orbitrap fusion mass spectrometer coupled to a Dionex Ultimate 3000 ultra-high-performance liquid chromatography system (Thermo Scientific, USA). This approach, similar to Fourier transform ion cyclotron resonance mass spectrometer, has become instrumental for tracing organic matter in complex systems due to its ultra-high mass resolution and accuracy (Lin et al., 2012; Wang et al., 2022; Wu et al., 2019). Multiple ionization

modes were used: +ESI, -ESI, and + APPI. Chemical constituents were separated using a Thermo Hypersil 1.9 μm, 100 × 2.1 mm C18 column, with a 7 μL injection volume and a flow rate of 0.2 mL/min. The liquid chromatography conditions were as follows: solvent A - methanol, and solvent B - water, both containing 0.1 % formic acid. The initial proportion was 90 % B, decreasing to 40 % over 20 min, and reaching 0 % over the next 40 min, maintained for 10 min, followed by a 1-min restoration to 90 %, and a final 8-min hold. Mass spectrometer conditions included -ESI/+ESI mode: spray voltage, 3600/2600 V; sheath/auxiliary gas 20/8 Arb; ion transfer tube/vaporizer temperature 300/200 °C; +APPI mode: sheath/auxiliary/sweep gas 35/10/2 Arb; ion transfer tube/vaporizer temperature 350/200 °C.

The original data were processed for molecular formula extraction analysis following the previous method (Wang et al., 2022). Molecular formulas were assigned with a mass tolerance of ±2 ppm, considering C, H, O, N, and S elemental combinations with set upper limits for atom counts. Double bond equivalence (DBE) constraints and isotopic pattern matching were applied to ensure chemically reasonable assignments, and peaks present in blanks were discarded unless the sample-to-blank intensity ratio exceeded 5 times.

2.7. Microbial community sequencing

Microbial community analysis within the incubation system was performed using high-throughput quantitative sequencing of 16S rDNA. DNA extraction from culture samples was carried out using the MO BIO/PowerSoil DNA Isolation Kit following the kit's protocol. For quantitative microbiome profilin, microbial loads were estimated using spike-in-based microbiome profiling methods (Wang et al., 2020). After concentration measurement, 500 pg of synthetic chimeric DNA spikes were added to the DNA samples. Specific amplification of the V3-V4 region of bacterial 16S rDNA was conducted using primers 343F-798R (343F: TACGGRAGGCAGCAG and 798R: AGGGTATCTAATCCT). Library construction and sequencing (Illumina MiSeq, PE 2 × 300 bp) were performed by Hanyu Biotech Lab (Shanghai, China).

Raw Illumina fastq files were processed for quality filtering and taxonomic analysis using QIIME 2 (Bolyen et al., 2019). Briefly, after primer removal from imported sequences using Cutadapt, DADA2 was employed for filtering and denoising sequences, removing chimeras, identifying representative sequences of amplicon sequence variants (ASVs), and creating an ASV table (Callahan et al., 2016). The representative sequences of ASVs were taxonomically annotated and corrected for 16S rDNA copy numbers based on the bacterial rrnDB database (version 13.8), reflecting the absolute copy numbers of species in the samples. Functional prediction analysis of 16S rDNA results was conducted using PICRUSt2 (Douglas et al., 2020).

The raw sequencing data of genes obtained by Pacbio in this study have been submitted to the NODE database under Project ID OEP005359.

2.8. Statistical analysis

All nutrients, dissolved oxygen, pH, and cell abundance parameters were determined using triplicate parallel samples, with results comprising an average of three replicated measurements. Concentrations of DOC, DON, and DOS, as well as FDOM measurements, were obtained from the meaning of three independently measured parallel samples. Spearman correlation analysis was employed to compare ASVs with DOM in each sample. Network analysis, highlighting significant positive correlations between microbial ASVs and DOM molecules (relative abundance in total DOM) with $R \geq 0.6$ and $P < 0.05$, was conducted using Python. Visualization of network analysis was performed in Gephi version 10.0.0. Canonical correspondence analysis (CCA) was executed using the 'vegan' package, the upset analysis was executed using the 'upsetR' package in R 4.3.3 (www.R-project.org). Visualizations of other data were carried out using OriginPro 2022b (OriginLab, MA, USA).

3. Results

3.1. Environmental changes in culture systems and growth of heterotrophic bacteria

Throughout the 7-day of incubation, the DP and P group exhibited distinct changes, particularly in physicochemical parameters (Fig. S1) and the concentrations of different types of OC, including DOC, DON, and DOS (Fig. 2). Heterotrophic bacteria grew slower in the hypoxic culture compared to the P group, with a 48-h lag in reaching the saturation growth phase. However, both systems were enriched with readily utilized algal-derived OC, which facilitated bacterial growth from 10^5 cells/mL to a high population density of 10^7 cells/mL. High OC concentrations and initial DO provided a rapid growth environment for the oxygen-consuming group. This led to a swift decline in DO levels (reaching hypoxic levels of DO <5 μmol/L within 48 h) and an intensified assimilation of nitrogen due to increased biomass, resulting in rapid nutrient consumption. In both conditions, ammonium concentrations increased during periods of microbial proliferation and rapid DON decrease.

Under conditions with 8 times increase in initial carbon source concentration, both the DP and P groups showed a rapid decline in DOC and DON concentrations within the first 24 h, while DOS remained relatively stable under hypoxia (Fig. 2 a, d, and g). Specifically, DOC consumption in the P group was 2.42 times higher than in the DP group during the first 24 h (DOC consumption increased from 17.89 ± 2.69 % in the DP group to 43.46 ± 8.78 % in the P group), with 67.11 ± 7.26 % and 96.01 ± 1.80 % of DON being utilized in hypoxic and oxygen-consuming incubations, respectively. The proportion of DOS consumed in the DP group within 48 h was only 7.17 ± 3.55 %.

The calculated early-stage consumption rates further emphasize this difference, especially for DON, which was higher under P group (Fig. 2 b, e, and h). By the end of the experimental period, the added DOC concentrations were nearly equal in both groups, with DOC consumption percentages at 62.5 ± 7.7 % for DP and 65.9 ± 2.7 % for P groups. The results reveal that DON is the preferred OC fraction for heterotrophic bacterial metabolism in both groups, whereas DOS remains more stable under hypoxia conditions.

Although DO limitation temporarily slowed DOC utilization under hypoxia, the total amount consumed over the 7-day period was comparable between the groups. The slower microbial growth in the DP group resulted in reduced DOC turnover rates during the early phase. Linear relationships were observed between microbial cell growth and the consumption of DOC, DON, and DOS (Fig. 2c, f, and i), with a particularly strong correlation between growth and DON utilization under hypoxic conditions. These slopes reflect the adaptive metabolic responses of microbial communities to oxygen limitation. Overall, the results highlight substrate-specific consumption patterns, microbial metabolic rates, and growth–substrate coupling in response to varying degrees of hypoxia.

3.2. Microbial community stress and succession in the system

During the incubation, 16S rDNA sequencing results showed that heterotrophic *Proteobacteria*, *Bacteroidetes* and *Firmicutes* dominated the abundance in both hypoxic and oxygen-consuming conditions in later stages after the addition of ADOM. *Flavobacteriaceae* exhibited one of the most notable increases in relative abundance during the incubation, rising from 6.1 ± 5.4 % on day 1 to 48.0 ± 8.3 % on day 7 in the treatment group (Fig. 3 a), showing no growth difference between the two groups, with the highest relative abundance observed on day 7 ADOM addition. *Rhodobacteraceae* reached high relative abundances on day 2, maintaining this level until day 7. *Vibrionaceae* displayed high relative abundance in the DP group on day 2, significantly higher than in

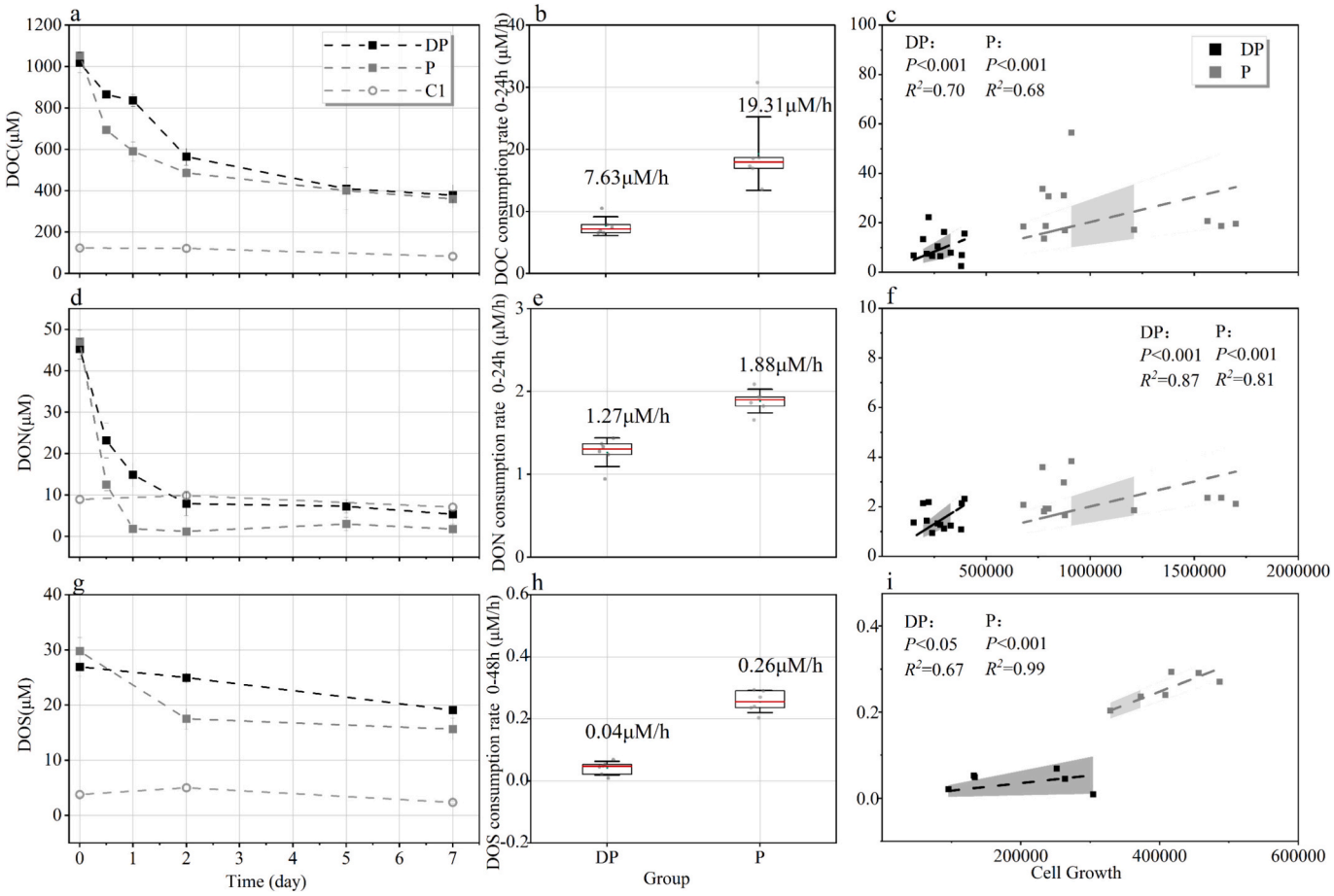


Fig. 2. Temporal dynamics, consumption rates, and growth-coupled responses of microbial communities to different organic compounds under hypoxic (DP) and oxygen-consuming (P) conditions. Panels a, d, g: The concentration changes of DOC, DON, and DOS, respectively, over a 7-day incubation period. These time-course plots illustrate distinct patterns of organic compound utilization between treatment groups. Panels b, e, h show the initial consumption rates of DOC, DON (0–24 h), and DOS (0–48 h) for each group, derived from the early-stage depletion data. Panels c, f, i present the linear relationships between microbial cell growth and the consumption of DOC, DON, and DOS, respectively. Shaded areas represent 95 % confidence intervals of regression. Significant correlations indicate the extent to which microbial proliferation is linked to specific substrate utilization under different oxygen regimes.

the P group at the same time but declined over time in the DP group. *Campylobacteraceae* and *Acidaminobacteraceae* also peaked on day 2 and subsequently declined. At the ASV level, as oxygen levels decreased in the P group, the community structure uniqueness shifted towards the hypoxic group, increasing shared microbial taxa and the PCA results in bacteria community composition gradually converged (Fig. S2).

Metabolic profiling focused on the relative abundance changes in amino acid metabolism, carbohydrate metabolism, and energy metabolism pathways (Fig. 3 b). Although no statistically significant differences were observed between the experimental groups, some temporal trends were still apparent over the course of the incubation. On day 0 and day 2 of the hypoxic incubation, the relative abundances of amino acid and lipid metabolism pathways were generally lower compared to the P group, with DP:P relative abundance ratios of 0.954 and 0.908, respectively, on day 2. However, by day 7, these trends reversed: amino acid and lipid metabolism under hypoxic conditions exceeded those under P group, with ratios increasing to 1.034 and 1.032, respectively. The most pronounced change was observed in chemical structure transformation pathways, where the ratio increased from 0.515 on day 2 to 1.505 on day 7.

The community and metabolic predictive changes demonstrated that the P group, as the incubation time progressed, increasingly resembled the microbial features observed and altered under continuous hypoxic conditions. Within 48 h, influenced by DO levels, larger changes in community and metabolism were observed, with a more substantial alteration of family-level community structures occurring as DO decreased. Regardless of the oxygenation status, heterotrophic bacteria consistently responded to OC. In the early stage of culture (day 0–2), however, cell proliferation and the abundance of metabolic pathways are constrained by oxygen concentration, some metabolic functions under hypoxia proceed more slowly compared to oxygen-consuming conditions. Longer incubation periods resulted in more aligned microbial communities and metabolism.

3.3. *Changes in fluorescent organic matter components*

PARAFAC identified four distinct fluorescent groups (C1, C2, C3, C4) (Fig. 4a). Comparison with the OpenFluor database indicated that C1 closely matched the $C_{320/422}$ component reported by Chen et al. (Chen et al., 2018), suggesting that this type of FDOM likely originates from *in situ* marine production. C2 resembled terrestrial humic-like components (Hong et al., 2021; Lambert et al., 2016), which are typically associated with photochemically mediated production, photorefractory materials, or terrestrial inputs. C3, another humic-like substance (Lambert et al., 2016; Lapierre and del Giorgio, 2014), exhibited strong photosensitivity, typically being completely removed after 12–24 h of irradiation. C4 corresponded to freshly produced protein-like material (Guillemette and del Giorgio, 2011; Yamashita et al., 2010), prevalent in bioproduction processes and readily degradable by microbes at nutrient-rich sites.

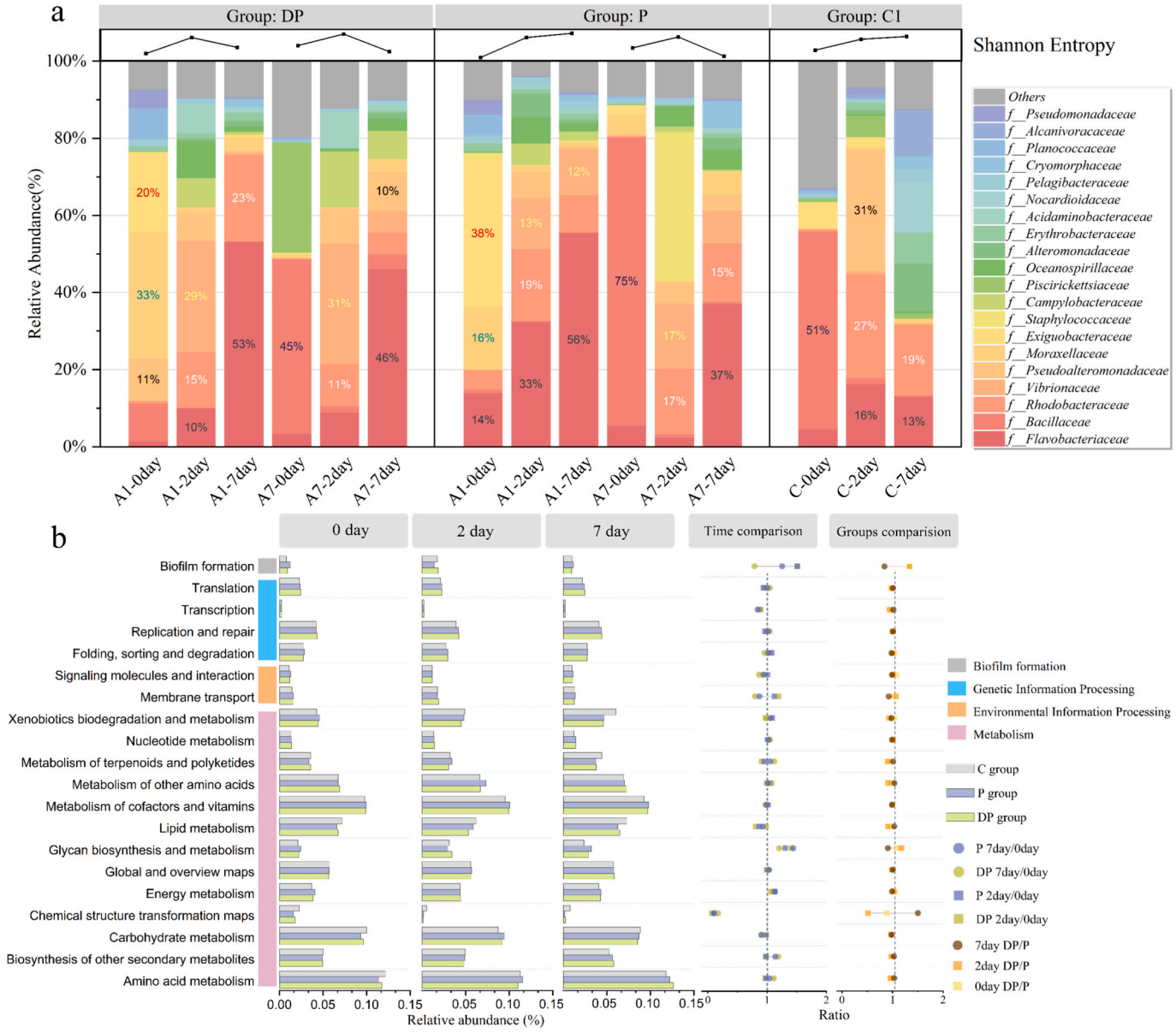


Fig. 3. Dynamic changes in microbial community and metabolic pathway. a. Relative abundance of microbial taxa at the family level across different samples, along with changes in Shannon entropy index for each sample. b. Metabolic pathway variations across time points and treatment groups, respectively presenting the relative abundance of various metabolic pathways in the P, DP, and Control groups at three different time points (0 days, 2 days, 7 days); the abundance change ratios of metabolic pathways in the P and DP groups at different time points; and the abundance ratio differences of metabolic pathways between the two groups at the same time point.

Among the identified fluorescent components, humic-like C1 and C2 showed minimal changes in signal intensity in both experimental groups. In contrast, C3 displayed significant increases in fluorescence under the P group, differing notably from the DP group and control. C4 rapidly declined within 48 h in both groups, with a more pronounced decline observed under oxygen-consuming conditions (Fig. 4.b). This decline correlated with a decrease in DON concentrations($R^2 = 0.726$, $p < 0.001$) (Fig. S3). The fluorescence spectral slope ratio (SR) (The spectral slope over 350–400 nm) and SUVa254(specific ultraviolet absorbance at 254 nm) indices revealed an increase in the aromaticity of FDOM and a reduction in average molecular weight(Fig. 4.c).

3.4. Analysis of organic carbon molecular fingerprints

Molecular formula analysis of the samples revealed an increase in sulfur-containing aromatic compounds following hypoxic incubation (Fig. 5a). The proportion of CHONS/CHOS components in bottom waters from different stations increased after hypoxic incubation with added ADOM. Although the relative abundance of CHOS molecules also increased in the control group over the 7-day incubation, the increase (2.95 %) was smaller than that observed in the DP group, where CHOS abundance increased by 4.67–6.94 %. Due to limited sample size, statistical significance could not be determined; however, the observed trend suggests a greater CHOS accumulation under deoxygenated conditions. However, characteristics such as CHO, O/C ratio, and DBE decreased. Redox changes in SPE-DOM organic components were more pronounced under hypoxia. This coincided with a concurrent increase in the relative abundance of carboxyl-rich alicyclic molecules (CRAM) (Fig. 5a). Analysis of key DOC-SPE molecules revealed the addition of ADOM introduced 384 new molecular formulas (Fig. 5b). These formulas were predominantly in the aliphatic category and included numerous CHON and CHOS molecules. However, only a small fraction

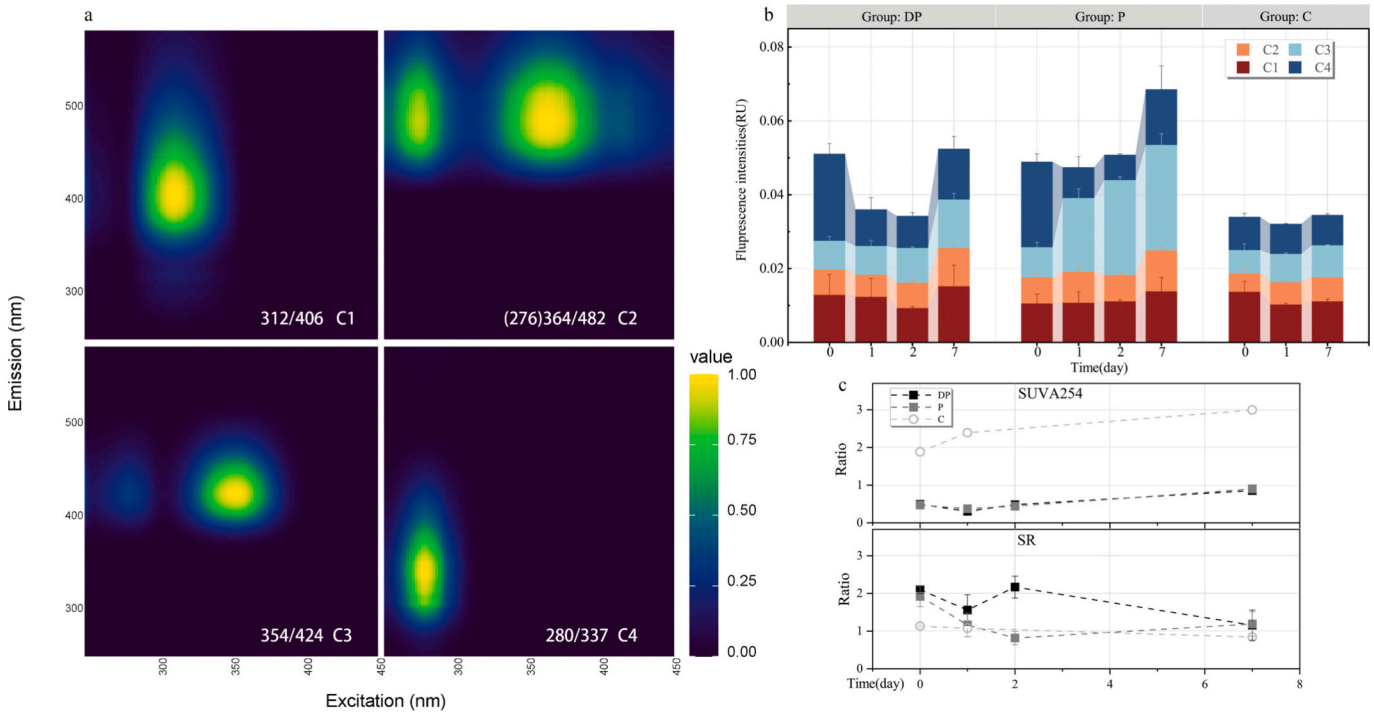


Fig. 4. Fluorescence Characteristics and Temporal Variation of Specified Compounds in Different Groups. a. fluorescent group features of the four distinct substances (C1, C2, C3, C4) identified through PARAFAC; b. Changes in fluorescence intensity of the four fluorescent FDOM compounds at different time points across various groups; c. Temporal variation trends of the two parameters, SUVA254 and SR, for FDOM during the experiment.

of molecules in the added components of ADOM belong to the CRAM. Following cultivation under both experimental conditions, new molecular formulas emerged. Hypoxic conditions displayed a greater variety of new formulas (336) compared to oxygen-consuming conditions (270). These new formulas encompassed CHONS molecules within the aliphatic category and CHOS molecules within the aromatic category. Additionally, concentrated clusters of CRAM molecules were observed in both groups. The added ADOM introduced new algae-derived molecules, including 148 formulas of CHO and 150 formulas of CHON molecules (Fig. 5c). Compared to the P group, more CHOS molecules were produced after culture in the DP group (DP/P: 102/62), and more CHO molecular were depleted (DP/P: 120/80). Under different culture conditions, only a few formulas of CHO molecules were produced, while more OC containing nitrogen and sulfur was generated.

From the consumption perspective, the analysis of molecular groups completely depleted after the experiments showed consistent characteristics across groups. The DP group exhibited the most various depletion, exhausting more molecular formulas (Fig. 5 c), with 174 molecules consumed by both the DP and P groups in shared. A total of 1478 molecular types were present in the samples across all culture stages, with only 142 molecules produced by both the DP and P groups overlapping. In control groups, a significant amount of *in situ* CHO and CRAM substances disappeared following cultivation. The completely transformed molecular fractions predominantly centered around 600 *m/z* and were mainly composed of CHON groups (Fig. S4). Low m/z SPE-DOM molecules were categorized as belonging to aromatic, carbohydrates, and lignin CRAM classes. Conversely, the depleted high m/z molecules were mostly tannin or protein aliphatic. Compared to the C group, the addition of algal sources in the experimental groups led to the depletion of numerous CHON molecules. Moreover, larger m/z CHO molecules also disappeared within the cultivation system.

3.5. Microbial-organic carbon coupling analysis

CCA revealed relationships between DOM component parameters, environmental factors, and microbial communities across different cultivation times (Fig. 6a). Concentrations of DON, DOC, and FDOM component C4, along with the SR, significantly impacted early-stage microbial communities. Among other environmental factors, variations in nutrients had the strongest influence on the initial community structure. In samples collected on days 2 and 7, components C2, C3, ammonium concentration, and community abundance indices showed correlations with the corresponding microbial communities.

Network analysis further elucidated relationships between key microbial communities (relative abundance above 0.1 %) and major SPE-DOM molecules (intensity above 0.005 %) under hypoxic and oxygen-consuming conditions (Fig. 6b). Two distinct network patterns emerged across the experimental groups. In the DP group, links between microbes and molecules were fewer than in the P group, with more negative relationships (55.77 %) in the P group. Key microbial nodes links in the DP group were mainly *Hyphomicrobiaceae* and *Exiguobacteraceae*, while in the P group, *Micrococcaceae*, and *Exiguobacteraceae* prevailed. A unique microbe-organic molecule module associated with positive correlations with DOS molecules emerged in hypoxic incubation, primarily involving *Shewanellaceae* and *Bacteroidetes*. In oxygen-consuming conditions, two separate modules emerged, mainly linking DON with microbes. Further dissection of network relationships revealed key links and nodes in both conditions, with CHON, CHOS, and CHONS molecules in the DP group showing more significant positive correlations ($P < 0.05$, $R > 0.6$) compared to CHO molecules (Fig. 6c). This indicates a potential relationship between key microbial groups adapted to deoxygenation and OC containing nitrogen and sulfur.

4. Discussion

4.1. The impact of limited DO on heterotrophic microbial utilization of DOC in the ocean

Marine heterotrophic microorganisms respond rapidly to ADOM during coastal eutrophication-induced algal blooms, contributing fresh,

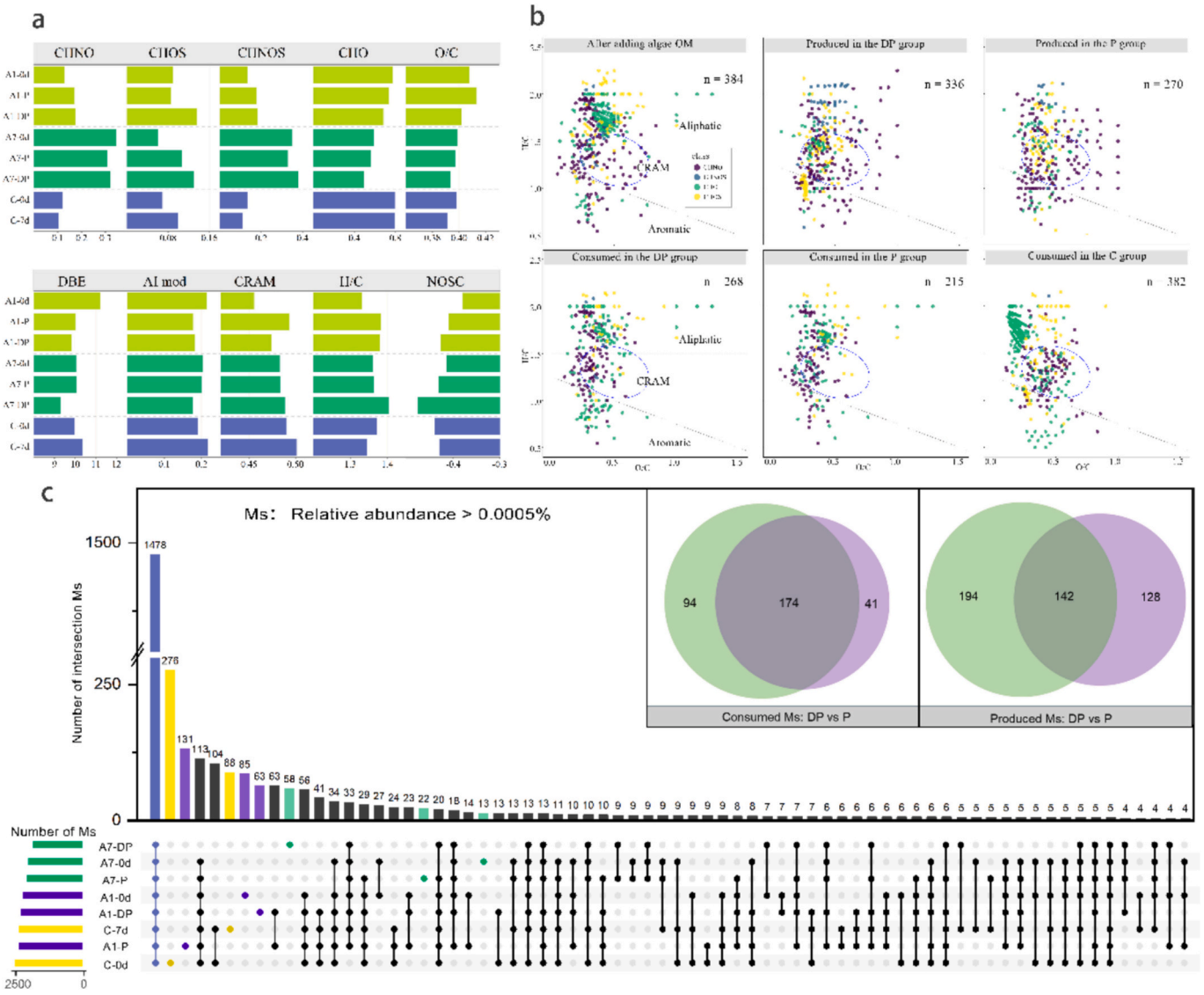


Fig. 5. Changes in chemical compositions and organic compounds distribution under different conditions. a. This panel shows the changing characteristics of different chemical compositions (*e.g.*, CHNO, CHOS, CHNOS, CHO) of SPE-DOC molecules throughout the cultivation process. Additionally, it displays the corresponding chemical parameters of the measured compositions (such as O/C, DBE, AI mod, CRAM, H/C, NOSC, *etc.*). b. The Van Krevelen diagram depicts molecules with a relative intensity above 0.005 %, illustrating the features of the SPE-DOM molecules newly introduced after adding algal fluid, the newly formed SPE-DOM compositions after cultivation in different groups, and the SPE-DOM molecular features that completely disappear (or are exhausted) post-cultivation. c. Upset analysis shows the number of shared and different molecules between different samples (The top 0.005 % relative abundance molecules in each sample), and the Venn diagram shows the number of consumed and produced molecules between the DP and P groups. A1-0d/A7-0d represent the samples at day 0 after the addition of ADOM. A1-P/A7-P denote the samples from the P groups on day 7. A1-DP/A7-DP indicate the samples from the DP groups on day 7. C-0d and C-7d represent the C group samples at days 0 and 7, respectively.

nitrogen-rich DOC and polysaccharides that enhance DOM bioavailability and trigger microbial priming effects (He et al., 2022b; Jiao et al., 2011; Wang et al., 2017). In the Yangtze River Estuary, the interplay among hypoxia, microbial activity, and organic matter dynamics has been widely observed (Wang et al., 2016; Ye et al., 2016; Zhang et al., 2022). In our study, the addition of ADOM increased DOC concentrations by approximately 8 times - within the range (2–10 × *in situ* levels) reported during coastal algal blooms (Duan et al., 2015; Han et al., 2021; He et al., 2022b; Lyu et al., 2022). This experimental setup was designed to simulate microbial OC utilization following large LDOC inputs associated with bloom-driven deoxygenation and subsequent hypoxia.

Marine heterotrophic bacteria readily utilize ADOM, with roughly more than half being mineralized into CO_2 (released back into the environment) or incorporated into microbial biomass (Moran et al., 2022a). Our addition incubation experiments showed that under both hypoxic and oxygenated conditions, about 64.3 % of the DOC was consumed and transformed within seven days (Fig. 2 a). This fraction represents the most favored source of OC in ADOM by heterotrophic bacteria and contains a large amount of organic nitrogen (Moran et al., 2022b). However, the impact of DO on DOC transformation has been underexplored. Previous studies show that oxygen concentration directly affects the rate of microbial remineralization (Le Moigne et al., 2017; Massmig et al., 2020; Nguyen and Harvey, 1997). While hypoxia initially slows down DOC utilization (with oxygen supply increasing the rate by 2.4 times within 24 h), the final amount of DOC remaining is similar. This suggests that limited DO may not significantly restrict the bioavailability of DOC for heterotrophic bacteria. Instead, the observed weakening of marine priming effects under hypoxia likely results from the inhibited growth of most aerobic microorganisms (Couvert et al., 2019).

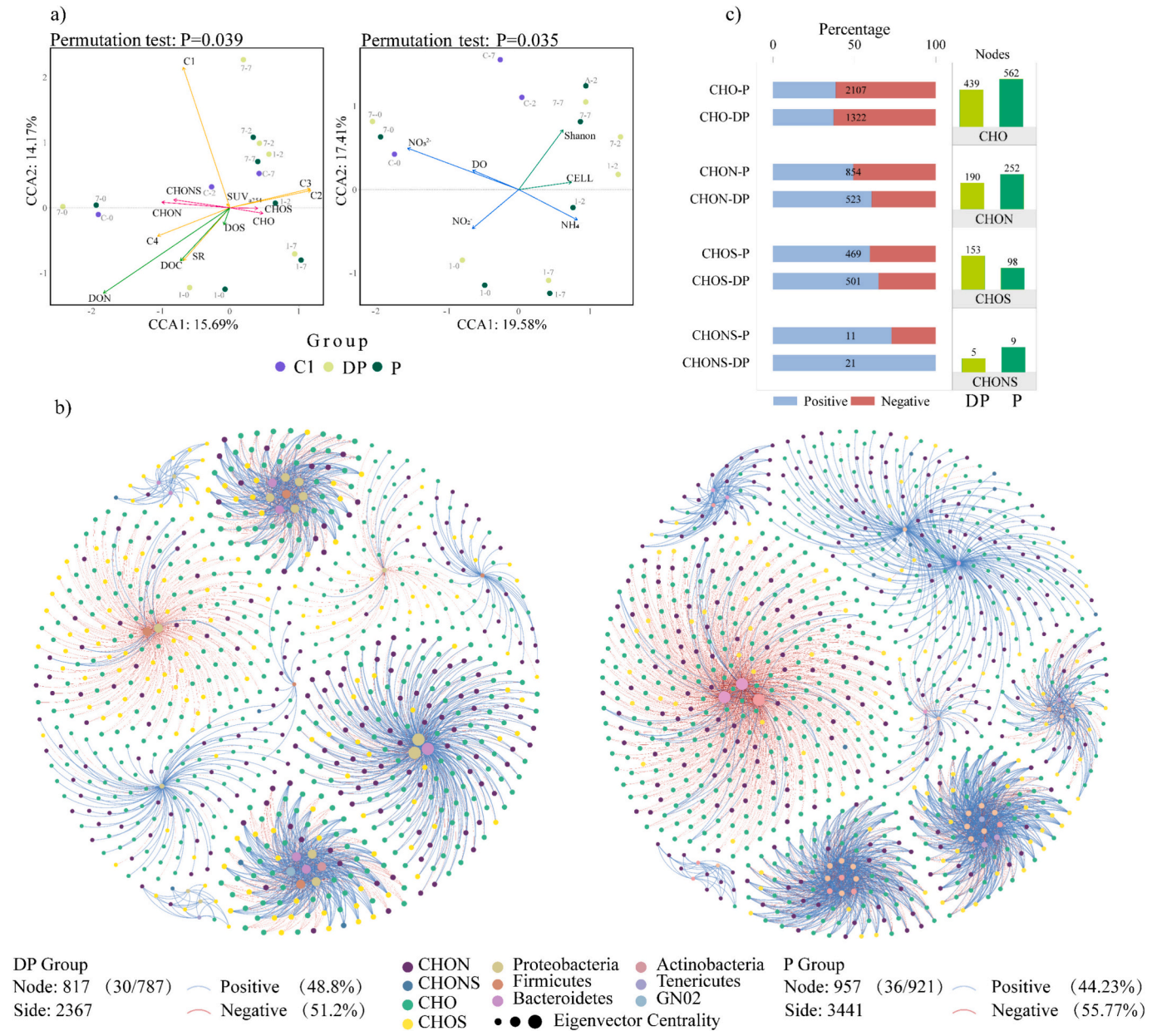


Fig. 6. Differences in microbial communities, organic matter composition, and environmental factors under various cultivation conditions. a. This panel displays a CCA analysis for samples at different time points. The CCA relates OC-associated parameters, environmental factors, microbial community and cellular metrics. b. This panel features the correlation network characteristics between the most abundant 0.1 % of microbes and SPE-DOM molecules (correlation threshold: $P < 0.05$, $R > 0.6$). The size of each node corresponds to its Eigenvector centrality, highlighting the importance of key microbial nodes within the network. This metric not only considers a node's direct connections (degree centrality) but also the centrality of its connected nodes. c. This panel reveals specific characteristics of the relationships between microbial entities, different types of SPE-DOM nodes, and edges, as determined by the network relationship analysis.

It is also proposed that high concentrations of LDOC inputs force microorganisms to allocate their limited metabolic capacity among multiple carbon sources, resulting in reduced utilization of certain DOC molecules (Wang et al., 2019). This phenomenon, referred to as substrate competition, occurs when microorganisms are exposed to a mixture of available substrates but cannot simultaneously process all of them with equal efficiency. As a result, they preferentially metabolize more labile or energetically favorable compounds (Mcnichol et al., 2024)—such as specific amino acids or nitrogen-rich DOC—while others are left underutilized. Under oxygenated conditions, microbial metabolism is generally more efficient, whereas substrate competition may intensify under hypoxic conditions, where energy yield per substrate is lower and enzymatic capacity may be limited (Giovannoni et al., 2021). This theory may partially explain the observed preservation of some algal-derived DOC under low-oxygen conditions. Our results suggest that the addition of ADOM may have triggered substrate competition, potentially reducing the microbial utilization of native DOC.

In this study, a limited amount of DON and DOS was preserved under hypoxic conditions, which correlates with the reduced decomposition rate of certain protein-like substances in low-oxygen environments, consistent with previous reports (Pantoja et al., 2009). Previous studies suggested that DON degradation might actually be enhanced in low oxygen and anoxic water masses (Pantoja et al., 2004), our results showed weaker DON transformation under short-term but severely hypoxic conditions. This may be due to the near-complete depletion of oxygen, which suppresses the activity of aerobic heterotrophs typically involved in DON turnover. Additionally, influenced by abiotic and biotic sulfidation under hypoxia, the degradation rate of DOS differs more

significantly from DON and DOC in relation to heterotrophic bacterial growth (Fig. 2c, f, and i). Some past researches showed hypoxia conditions could contribute to the generation of new DOS formation in the laboratory, which was subsequently discussed in detail, and a framework for DOS storage under hypoxia was proposed (Chen et al., 2022a; Pohlabeln et al., 2017). This discovery emphasizes that the total amount of OC remaining is similar in situations with a significant influx of ADOM, leading to deoxygenation, or in continuous hypoxic water columns. In these scenarios, the growth rate of heterotrophic microorganisms under hypoxia or their response time to OC appears to be the limiting factor. Similar patterns have also been reported for algal-derived DOM. For instance, recent incubation experiments demonstrated that marine anoxia significantly hinders the transformation of kelp-derived DOC into RDOC, resulting in lower conversion efficiency compared to normoxic conditions(Zhao et al., 2025b). Together with other studies showing that macroalgal biomass conversion to RDOC is reduced under anoxia (Zhao et al., 2025a), these findings highlight the broader role of oxygen availability in regulating the microbial transformation and long-term preservation of algal-derived DOC.

4.2. Metabolic differentiation and convergence under deoxygenation and hypoxia

Coastal eutrophication and algal blooms can lead to deoxygenation in bottom waters, exhibit divergent microbial ecological functions compared to oxygenated waters and sediments. Previous study has highlighted that these metabolic differences are particularly pronounced in anoxic water columns (Spietz et al., 2015). However, the response of some “opportunistic” bacteria to ADOM was not significantly inhibited at deoxygenated-even microaerobic levels in this study, such as *Flavobacteriaceae*, *Pseudoalteromonas*, and *Alteromonas* (Fig. 3 a), It is generally believed that these bacteria are widespread in algal blooms and deoxygenation or even anoxic environments (Han et al., 2021; Zheng et al., 2020). Also, in hypoxia or anaerobic waters, both aerobic and anaerobic microbial processes can occur simultaneously (Bertagnolli and Stewart, 2018). While bacteria that extensively utilize DOC consistently dominant OC remineralization across various systems, their predominance under hypoxic and deoxygenated conditions suggests a strong adaptability to deoxygenation environments, a common characteristic of many heterotrophic bacteria (Long et al., 2021). However, studies have also shown that sustained hypoxia can lead to the emergence of distinct microbial communities, particularly among oxygen-sensitive anaerobes or aerotolerant bacteria, such as *Arcobacter*, *Clostridiales*, *Desulfobulbaceae* under hypoxic conditions (J.V. Sinu, 2022; Yu et al., 2023). A Study on simplified metabolic models for aerobic microorganisms in marine oxygen minimum zones suggests that a DO range of 0.1–10 nM can act as a dynamic survival oxygen threshold for aerobic microbial metabolism (Zakem and Follows, 2017). This considerably low oxygen content implies that most heterotrophic bacteria can survive in deoxygenated aquatic environments, with their differences primarily reflected in growth metabolism and organic matter consumption.

This study revealed the enrichment of microbial pathways for nitrogen and sulfur metabolism, as well as oxidative phosphorylation, during the early stages of hypoxic incubation compared to deoxygenated conditions. This finding supports the prevalence and rapid metabolic adaptation of active denitrification, anammox, and sulfur metabolism in hypoxic environments (Wright et al., 2012). Certain heterotrophic bacteria commonly found in deoxygenation waters exhibit variations in the ability to utilize oxygen through terminal oxidases (Murillo et al., 2014). Under hypoxia, when microbes encounter abundant OC, they tend to produce more biofilms, especially when *Flavobacterium*—a genus known for its biofilm-forming capability—is prevalent (Magesh et al., 2024). These biofilms form particulate organic carbon components that can envelop some organic matter, limiting its exposure to extracellular enzymes (Ploug et al., 1997). This coincides with the observed higher abundance of genes related to biofilm formation under hypoxia (Fig. 3 b). Biofilm formation may facilitate the burial of refractory carbon by embedding organic matter within extracellular polymeric substances, which can reduce microbial access and degradation (Duteil et al., 2022). Under hypoxic conditions, such microbial biofilms are more likely to persist, enhancing organic carbon stabilization in the environment (Cabrera-Brufau et al., 2021).

Furthermore, some studies have explored amino acid recycling and *in situ* degradation in hypoxic water(Pantoja et al., 2009; Vandewiele et al., 2009). The study revealed that under high OC input, microbial communities play a more significant role in fatty acid and D-amino acid metabolic pathways during oxygen-consuming processes compared to hypoxia. Pathways such as glycan biosynthesis and metabolism, lipid metabolism, and D-amino acid metabolism were more impacted, including glycosaminoglycan degradation, lipopolysaccharide biosynthesis, peptidoglycan biosynthesis, linoleic acid metabolism, and sphingolipid metabolism (Fig. 3 b). The availability of DO still partially restricted these pathways, this findings are consistent with research results in the Arabian Sea's oxygen minimum zones (Vandewiele et al., 2009). These nitrogen metabolic processes, influenced by oxygen limitation, may explain why the N:C ratio in DOC during hypoxic incubation is higher than during deoxygenated incubation.

These metabolic processes differences were most evident in the initial stages of oxygen-consuming and hypoxic cultivation, reflecting subtle variations in microbial metabolic strategies. However, as oxygen depleted in the cultivation system, microbial metabolic potential tended to converge. This aligns with the observed stability of heterotrophic bacterial communities in the later stages of cultivation, suggesting a convergence towards a shared metabolic state, Therefore, there is more overlap between the final microbial community and molecular diversity.

4.3. Molecular type consumption of ADOM under deoxygenation and anoxia

In addition to the mineralization of OC into CO_2 and its conversion into autogenic biomass, marine microbial transformation of organic matter involve a process known as the microbial carbon pump(MCP), where LDOC is transformed into refractory DOC by microbes (Jiao et al., 2010). Extensive research, including cultivation and field studies, has focused on optical properties, molecular composition, and even molecular structure of OC (He et al., 2022a; Xiao et al., 2023; Zhao et al., 2019). The rate of microbial degradation and transformation of OC depends on the substrate's molecular composition and size (Amon and Benner, 1996). Recent experimental evidence indicates that under anoxic conditions, only approximately 5 % of macroalgal-derived LDOC was converted to RDOC, compared to approximately 9 % under oxygenated conditions (Zhao et al., 2025a). This study found that the concentration of the remaining DOC after cultivation was relatively similar, indicating that microbes could mineralize most LDOC within a short period, consistent with findings in anoxic natural environments (Chen et al., 2022b). The depleted DOC molecules were predominantly composed of CHON, followed by CHO. The rapid decrease in protein-like components of FDOM, the degradation rate of DON, and the exhaustion of CHON molecules all indicate that microbial degradation of nitrogen-containing compounds can proceed rapidly even under limited oxygen conditions (Chen et al., 2022b). This result is consistent with active amino acid metabolism in microbial metabolism. The initially elevated signal of the C4 fraction may be attributed to fresh protein-like material present in the added ADOM. Additionally, viral lysis of microbial cells could have released accumulated protein-like compounds generated during the microbial transformation of ADOM (Chen et al., 2024; Zheng et al., 2021), potentially contributing to the increased C4 fluorescence observed on day 7 (Fig. 4 b). The higher relative proportion of positive correlations between bacterial communities and CHON under hypoxic cultivation also suggests the potential for partial preservation of DON with oxygen depletion (Fig. 6). This is further supported by evidence of

total hydrolyzable amino acid accumulation in anoxic stations of the Black Sea (Jessen et al., 2017). This study also observed that microorganisms produced more organic molecules with nitrogen- and sulfur-containing after 7 days of culture.

Consistent with our findings, previous studies have shown that the addition of ADOM leads to the rapid production of relatively abundant and recalcitrant CRAM substances and humic-like components by microbes under both deoxygenation and hypoxic conditions (Hertkorn et al., 2006; Yamashita and Tanoue, 2008). However, the control group also showed some microbial consumption of CRAM substances present in the background seawater, similar to observations in pure culture experiments (Liu et al., 2020). This background pool of CRAM may partly originate from *in situ* production by estuarine vegetation, such as macroalgae and seagrasses, which have been shown to release refractory DOC with humic-like optical features (Egea et al., 2023; Kubo and Tanaka, 2023). A study also revealed that ADOM produces more nitrogen-containing CRAM after microbial metabolism in the trench sediment(Chen et al., 2023). These findings suggest that not all CRAM materials effectively resist microbial utilization, and further investigation is needed to determine the factors influencing their persistence.

Previous studies in anoxic Black Sea sediments report a 3 times increase in sulfur-containing compounds (CHOS and CHONS) in pore water compared to oxygenated bottom water. Additionally, anoxic water masses exhibit 2–3 times increase in the burial chlorophyll pigments, suggesting that some ADOM is preserved under anoxic conditions (Jessen et al., 2017). Recent research supports the concept of consistent organic matter sulfidation and burial in deoxygenated oceans (Raven et al., 2021a, 2021b). Despite the short cultivation period and limited duration of hypoxia, DOS consumption was significantly suppressed under hypoxia in this experiment. This study found that, unlike carbohydrates or nitrogenous organic matter, microbial responses towards DOS rapidly diverged under hypoxia. Furthermore, after the hypoxic phase, CHOS and CHONS characteristics in DOC-SPE revealed production, stronger positive correlations with specific microbial communities, and significant network modular differentiation.

Our study revealed an increase in the sulfur content of organic matter, with S:C ratio rising from 2.64 % pre-cultivation to 5.04 % post-cultivation under hypoxia. The same sulfurization phenomenon does not only occur in anaerobic sediments(Dong et al., 2024), its also corroborated by findings in the Black Sea, where environments are completely anoxic and sulfurized had high levels of DOS produced by microbes, this sulfur-rich organic matter accumulated in the water column (Gomez-Saez et al., 2021). These results highlight that the sulfurization of OC under hypoxia can occur not only in long-term stable sediments but also rapidly due to microbial metabolism. This underscores the need for further investigation into the interactions between sulfur-metabolizing microbes, anoxic environments, and carbon sequestration.

In conclusion, this study tested the hypothesis that microbial communities in the Yangtze River Estuary possess metabolic plasticity under oxygen-limited conditions. Our incubation experiments confirmed that although hypoxia initially suppressed the microbial utilization rate of ADOM, particularly for DOC, overall carbon processing capacity remained comparable to oxygenated conditions over time, supporting the idea of community-level adaptation. We found that DON consistently the most efficiently utilized fraction, with strong correlations to microbial growth under both deoxygenated and oxygen-consuming conditions, indicating its central role in driving heterotrophic activity. In contrast, DOS remained largely stable under hypoxia, exhibiting distinct microbial associations and redox-sensitive transformation patterns. Community analyses revealed that heterotrophic bacterial families such as *Flavobacteriaceae*, *Rhodobacteraceae*, and *Pseudomonadaceae* dominated under both conditions but exhibited temporal shifts in abundance and metabolism, converging over time as oxygen levels declined. These results demonstrate that deoxygenation-anoxia alters not only the rate but also the nature of microbial OC transformation. Our findings clarify the dynamic limits of OC metabolism in coastal microbial communities and uncover how microbial structure, metabolic function, and substrate preference adapt under hypoxic stress. This study also has certain limitations, the potential bottle effects cannot be entirely excluded, although these factors are unlikely to alter the overall trends reported here. This work provides mechanistic insights into the microbial processing of algal-derived OC in seasonally hypoxic estuaries, advancing our understanding of how coastal deoxygenation shapes carbon cycling at the ecosystem scale. Future studies should consider isotopic labeling approaches (*e.g.*, with ^{13}C-labeled ADOM) to trace the incorporation of algal carbon into microbial biomass or its transformation into refractory forms. Such methods will be critical for better constraining the long-term implications of coastal hypoxia on microbial carbon storage efficiency.

CRediT authorship contribution statement

Quanrui Chen: Writing – original draft, Visualization, Investigation, Formal analysis. **Changjie Dong:** Investigation. **Yuguo Li:** Formal analysis. **Quan Shi:** Writing – review & editing, Methodology. **Xiaoxia Chen:** Writing – review & editing, Formal analysis. **Kai Tang:** Writing – review & editing, Supervision, Conceptualization. **Nianzhi Jiao:** Writing – review & editing, Supervision, Funding acquisition.

Declaration of competing interest

The authors declare that they have no known competing financial interests or personal relationships that could have appeared to influence the work reported in this paper.

Acknowledgments

This work is supported by the National Key Research and Development Program of China (2020YFA0608300), the National Natural Science Foundation of China project (92251306, 42141003, 42188102), the Ministry of Science and Technology (MOST) ONCE project.

Appendix A. Supplementary data

Supplementary data to this article can be found online at https://doi.org/10.1016/j.marpolbul.2025.118684.

Data availability

Data will be made available on request.

References

Amon, R.M.W., Benner, R., 1996. Bacterial utilization of different size classes of dissolved organic matter. Limnol. Oceanogr. 41, 41–51. https://doi.org/10.4319/lo.1996.41.1.0041.

Baroni, I.R., Palastanga, V., Slomp, C.P., 2020. Enhanced organic carbon burial in sediments of oxygen minimum zones upon ocean deoxygenation. Front. Mar. Sci. 6. https://doi.org/10.3389/fmars.2019.00839.

Bertagnolli, A.D., Stewart, F.J., 2018. Microbial niches in marine oxygen minimum zones. Nat. Rev. Microbiol. 16, 723–729. https://doi.org/10.1038/s41579-018-0087-z.

Bolyen, E., Rideout, J.R., Dillon, M.R., Bokulich, N., Abnet, C.C., Al-Ghalith, G.A., et al., 2019. Reproducible, interactive, scalable and extensible microbiome data science using QIIME 2. Nat. Biotechnol. 37, 852–857. https://doi.org/10.1038/s41587-019-0209-9.

Breitburg, D., Levin, L.A., Oschlies, A., Grégoire, M., Chavez, F.P., Conley, D.J., et al., 2018. Declining oxygen in the global ocean and coastal waters. Science 359, eaam7240. https://doi.org/10.1126/science.aam7240.

Cabrera-Brufau, M., Arin, L., Sala, M.M., Cermeño, P., Marrasé, C., 2021. Diatom dominance enhances resistance of Phytoplanktonic POM to mesopelagic microbial decomposition. Front. Mar. Sci. 8. https://doi.org/10.3389/fmars.2021.683354.

Callahan, B.J., McMurdie, P.J., Rosen, M.J., Han, A.W., Johnson, A.J.A., Holmes, S.P., 2016. DADA2: high-resolution sample inference from Illumina amplicon data. Nat. Methods 13, 581. https://doi.org/10.1038/Nmeth.3869.

Chen, B.K., Liu, J.H., Xu, G., Li, G., 2021. Lowering pO2 interacts with photoperiod to alter physiological performance of the coastal diatom *Thalassiosira pseudonana*. Microorganisms 9. https://doi.org/10.3390/microorganisms9122541.

Chen, M., Park, M., Kim, J.H., Shinn, Y.J., Lee, Y.K., Hur, J., 2018. Exploring pore water biogeochemical characteristics as environmental monitoring proxies for a CO2 storage project in Pohang Basin, South Korea. Mar. Pollut. Bull. 137, 331–338. https://doi.org/10.1016/j.marpolbul.2018.10.036.

Chen, Q., Tang, K., Chen, X., Jiao, N., 2022a. Microbial sulfurization stimulates carbon sequestration in marine oxygen minimum zones. Sci. Bull. 67, 895–898. https://doi.org/10.1016/j.scib.2022.01.028.

Chen, Q., Lonborg, C., Chen, F., Zhang, R., Cai, R.H., Li, Y.Y., et al., 2024. Bottom-up and top-down controls on *Alteromonas macleodii* lead to different dissolved organic matter compositions. ISME Commun. 4. https://doi.org/10.1093/ismeco/ycae010.

Chen, X., Liu, J., Chen, J., Wang, J., Xiao, X., He, C., et al., 2022b. Oxygen availability driven trends in DOM molecular composition and reactivity in a seasonally stratified fjord. Water Res. 220, 118690. https://doi.org/10.1016/j.watres.2022.118690.

Chen, X.X., Cai, R.H., Zhuo, X.C., Chen, Q.R., He, C., Sun, J., et al., 2023. Niche differentiation of microbial community shapes vertical distribution of recalcitrant dissolved organic matter in deep-sea sediments. Environ. Int. 178. https://doi.org/10.1016/j.envint.2023.108080.

Couvert, O., Divanac'h, M.L., Lochardet, A., Thuault, D., Huchet, V., 2019. Modelling the effect of oxygen concentration on bacterial growth rates. Food Microbiol. 77, 21–25. https://doi.org/10.1016/j.fm.2018.08.005.

Dai, M., Zhao, Y., Chai, F., Chen, M., Chen, N., Chen, Y., et al., 2023. Persistent eutrophication and hypoxia in the coastal ocean. Cambridge Prisms: Coastal Futures 1, e19. https://doi.org/10.1017/cft.2023.7.

Diaz, R.J., Rosenberg, R., 2008. Spreading dead zones and consequences for marine ecosystems. Science 321, 926–929. https://doi.org/10.1126/science.1156401.

Dittmar, T., Koch, B., Hertkorn, N., Kattner, G., 2008. A simple and efficient method for the solid-phase extraction of dissolved organic matter (SPE-DOM) from seawater. Limnology and Oceanography-Methods 6, 230–235. https://doi.org/10.4319/lom.2008.6.230.

Dong, C., Chen, Q., Chen, J., Dong, L., Chen, Y., Jiao, N., et al., 2024. Investigating organic sulfur in estuarine and offshore environments: a combined field and cultivation approach. Sci. Total Environ. 926, 171599. https://doi.org/10.1016/j.scitotenv.2024.171599.

Douglas, G.M., Maffei, V.J., Zaneveld, J.R., Yurgel, S.N., Brown, J.R., Taylor, C.M., et al., 2020. PICRUSt2 for prediction of metagenome functions. Nat. Biotechnol. 38, 685–688. https://doi.org/10.1038/s41587-020-0548-6.

Duan, S.W., Chen, N.H., Kaushal, S.S., Chigbu, P., Ishaque, A., May, E., et al., 2015. Dynamics of dissolved organic carbon and total dissolved nitrogen in Maryland's coastal bays. Estuar. Coast. Shelf Sci. 164, 451–462. https://doi.org/10.1016/j.ecss.2015.08.004.

Duteil, T., Bourillot, R., Braissant, O., Grégoire, B., Leloup, M., Portier, E., et al., 2022. Preservation of exopolymeric substances in estuarine sediments. Front. Microbiol. 13. https://doi.org/10.3389/fmicb.2022.921154.

Egea, L.G., Jiménez-Ramos, R., Romera-Castillo, C., Casal-Porras, I., Bonet-Melia, P., Yamuza-Magdaleno, A., et al., 2023. Effect of marine heat waves on carbon metabolism, optical characterization, and bioavailability of dissolved organic carbon in coastal vegetated communities. Limnol. Oceanogr. 68, 467–482. https://doi.org/10.1002/lno.12286.

Engel, A., Kiko, R., Dengler, M., 2022. Organic matter supply and utilization in oxygen minimum zones. Annu. Rev. Mar. Sci. 14, 355–378. https://doi.org/10.1146/annurev-marine-041921-090849.

Giovannoni, S., Chan, F., Davis, E., Deutsch, C., Wolf, S., 2021. Biochemical barriers on the path to ocean anoxia? Mbio 12. https://doi.org/10.1128/mBio.01332-21.

Gomez-Saez, G.V., Dittmar, T., Holtappels, M., Pohlabeln, A.M., Lichtschlag, A., Schnetger, B., et al., 2021. Sulfurization of dissolved organic matter in the anoxic water column of the Black Sea. Sci. Adv. 7, eabf6199. https://doi.org/10.1126/sciadv.abf6199.

Guenet, B., Danger, M., Abbadie, L., Lacroix, G., 2010. Priming effect: bridging the gap between terrestrial and aquatic ecology. Ecology 91, 2850–2861. https://doi.org/10.1890/09-1968.1.

Guillemette, F., del Giorgio, P.A., 2011. Reconstructing the various facets of dissolved organic carbon bioavailability in freshwater ecosystems. Limnol. Oceanogr. 56, 734–748. https://doi.org/10.4319/lo.2011.56.2.0734.

Han, Y., Jiao, N.Z., Zhang, Y., Zhang, F., He, C., Liang, X.J., et al., 2021. Opportunistic bacteria with reduced genomes are effective competitors for organic nitrogen compounds in coastal dinoflagellate blooms. Microbiome 9, 71. https://doi.org/10.1186/s40168-021-01022-z.

Han, Y., Zhang, M., Chen, X.F., Zhai, W.D., Tan, E.H., Tang, K., 2022. Transcriptomic evidences for microbial carbon and nitrogen cycles in the deoxygenated seawaters of Bohai Sea. Environ. Int. 158. https://doi.org/10.1016/j.envint.2021.106889.

He, C., Liu, J., Wang, R., Li, Y., Zheng, Q., Jiao, F., et al., 2022a. Metagenomic evidence for the microbial transformation of carboxyl-rich alicyclic molecules: a long-term macrocosm experiment. Water Res. 216, 118281. https://doi.org/10.1016/j.watres.2022.118281.

He, D., Li, P.H., He, C., Wang, Y.T., Shi, Q., 2022b. Eutrophication and watershed characteristics shape changes in dissolved organic matter chemistry along two river-estuarine transects. Water Res. 214. https://doi.org/10.1016/j.watres.2022.118196.

Hertkorn, N., Benner, R., Frommberger, M., Schmitt-Kopplin, P., Witt, M., Kaiser, K., et al., 2006. Characterization of a major refractory component of marine dissolved organic matter. Geochim. Cosmochim. Acta 70, 2990–3010. https://doi.org/10.1016/j.gca.2006.03.021.

Holmes, R.M., Aminot, A., Kérouel, R., Hooker, B.A., Peterson, B.J., 1999. A simple and precise method for measuring ammonium in marine and freshwater ecosystems. Can. J. Fish. Aquat. Sci. 56, 1801–1808. https://doi.org/10.1139/cjfas-56-10-1801.

Hong, H.L., Wu, S.J., Wang, Q., Dai, M.Y., Qian, L., Zhu, H., et al., 2021. Fluorescent dissolved organic matter facilitates the phytoavailability of copper in the coastal wetlands influenced by artificial topography. Sci. Total Environ. 790. https://doi.org/10.1016/j.scitotenv.2021.147855.

Jessen, G.L., Lichtschlag, A., Ramette, A., Pantoja, S., Rossel, P.E., Schubert, C.J., et al., 2017. Hypoxia causes preservation of labile organic matter and changes seafloor microbial community composition (Black Sea). Sci. Adv. 3, e1601897. https://doi.org/10.1126/sciadv.1601897.

Jiang, Z.B., Chen, J.F., Zhou, F., Shou, L., Chen, Q.Z., Tao, B.Y., et al., 2015. Controlling factors of summer phytoplankton community in the Changjiang (Yangtze River) estuary and adjacent East China Sea shelf. Cont. Shelf Res. 101, 71–84. https://doi.org/10.1016/j.csr.2015.04.009.

Jiao, N., Herndl, G.J., Hansell, D.A., Benner, R., Kattner, G., Wilhelm, S.W., et al., 2010. Microbial production of recalcitrant dissolved organic matter: long-term carbon storage in the global ocean. Nat. Rev. Microbiol. 8, 593–599. https://doi.org/10.1038/nrmicro2386.

Jiao, N., Tang, K., Cai, H., Mao, Y., 2011. Increasing the microbial carbon sink in the sea by reducing chemical fertilization on the land. Nat. Rev. Microbiol. 9, 75. https://doi.org/10.1038/nrmicro2386-c2.

Katsev, S., Crowe, S.A., 2015. Organic carbon burial efficiencies in sediments: the power law of mineralization revisited. Geology 43, 607–610. https://doi.org/10.1130/G36626.1.

Keil, H., 1995. Sedimentary organic matter preservation: an assessment and speculative synthesis. Mar. Chem. 49, 137–139. https://doi.org/10.1016/0304-4203(95)00008-F.

Kubo, A., Tanaka, H., 2023. Recalcitrant dissolved organic carbon release and production from aquatic plants leachate. Mar. Pollut. Bull. 189. https://doi.org/10.1016/j.marpolbul.2023.114742.

Lambert, T., Bouillon, S., Darchambeau, F., Massicotte, P., Borges, A.V., 2016. Shift in the chemical composition of dissolved organic matter in the Congo River network. Biogeosciences 13, 5405–5420. https://doi.org/10.5194/bg-13-5405-2016.

Lapierre, J.F., del Giorgio, P.A., 2014. Partial coupling and differential regulation of biologically and photochemically labile dissolved organic carbon across boreal aquatic networks. Biogeosciences 11, 5969–5985. https://doi.org/10.5194/bg-11-5969-2014.

Le Moigne, F.A.C., Cisternas-Novoa, C., Piontek, J., Massmig, M., Engel, A., 2017. On the effect of low oxygen concentrations on bacterial degradation of sinking particles. Sci. Rep. 7. https://doi.org/10.1038/s41598-017-16903-3.

Li, G., Liu, J.X., Diao, Z.H., Jiang, X., Li, J.J., Ke, Z.X., et al., 2018. Subsurface low dissolved oxygen occurred at fresh- and saline-water intersection of the Pearl River estuary during the summer period. Mar. Pollut. Bull. 126, 585–591. https://doi.org/10.1016/j.marpolbul.2017.09.061.

Lin, P., Rincon, A.G., Kalberer, M., Yu, J.Z., 2012. Elemental composition of HULIS in the Pearl River Delta region, China: results inferred from positive and negative electrospray high resolution mass spectrometric data. Environ. Sci. Technol. 46, 7454–7462. https://doi.org/10.1021/es300285d.

Liu, S.J., Chen, Q.R., Liu, L., Dong, C.J., Qiu, X.Y., Tang, K., 2024a. Organic matter composition fluctuations disrupt free-living bacterial communities more than particle-associated bacterial communities in coastal waters. Sci. Total Environ. 949. https://doi.org/10.1016/j.scitotenv.2024.174845.

Liu, S.J., Hou, C.C., Dong, C.J., Zhao, D., Chen, Q.R., Yang, J.Y.T., et al., 2024b. Integrated multi-omics analyses reveal microbial community resilience to fluctuating low oxygen in the East China Sea. Environ. Res. 261. https://doi.org/10.1016/j.envres.2024.119764.

Liu, S.T., Parsons, R., Opalk, K., Baetge, N., Giovannoni, S., Bolaños, L.M., et al., 2020. Different carboxyl-rich alicyclic molecules proxy compounds select distinct bacterioplankton for oxidation of dissolved organic matter in the mesopelagic Sargasso Sea. Limnol. Oceanogr. 65, 1532–1553. https://doi.org/10.1002/lno.11405.

Long, A.M., Jurgensen, S.K., Petchel, A.R., Savoie, E.R., Brum, J.R., 2021. Microbial ecology of oxygen minimum zones Amidst Ocean deoxygenation. Front. Microbiol. 12. https://doi.org/10.3389/fmicb.2021.748961.

Lyu, L.A., Liang, H.R., Huang, Y.H., Ding, H.B., Yang, G.P., 2022. Annual hypoxia causing long-term seawater acidification: evidence from low-molecular-weight organic acids in the Changjiang estuary and its adjacent sea area. Sci. Total Environ. 818. https://doi.org/10.1016/j.scitotenv.2021.151819.

Magesh, S., Hurley, A.I., Nepper, J.F., Chevrette, M.G., Schrope, J.H., Li, C., et al., 2024. Surface colonization by Flavobacterium johnsoniae promotes its survival in a model microbial community. Mbio 15. https://doi.org/10.1128/mbio.03428-23.

Malviya, S., Scalco, E., Audic, S., Vincenta, F., Veluchamy, A., Poulain, J., et al., 2016. Insights into global diatom distribution and diversity in the world's ocean. PNAS 113, E1516–E1525. https://doi.org/10.1073/pnas.1509523113.

Marie, D., Partensky, F., Jacquet, S., Vaulot, D., 1997. Enumeration and cell cycle analysis of natural populations of marine picoplankton by flow cytometry using the nucleic acid stain SYBR green I. Appl. Environ. Microbiol. 63, 186–193. https://doi.org/10.1128/Aem.63.1.186-193.1997.

Massmig, M., Lüdke, J., Krahmann, G., Engel, A., 2020. Bacterial degradation activity in the eastern tropical South Pacific oxygen minimum zone. Biogeosciences 17, 215–230. https://doi.org/10.5194/bg-17-215-2020.

Mcnichol, S.M., Sanchez-Quete, F., Loeb, S.K., Teske, A.P., Walter, S.R.S., Mahmoudi, N., 2024. Dynamics of carbon substrate competition among heterotrophic microorganisms. ISME J. 18. https://doi.org/10.1093/ismejo/wrae018.

Moran, M.A., Ferrer-González, F.X., Fu, H., Nowinski, B., Olofsson, M., Powers, M.A., et al., 2022a. The ocean's labile DOC supply chain. Limnol. Oceanogr. 67, 1007–1021. https://doi.org/10.1002/lno.12053.

Moran, M.A., Kujawinski, E.B., Schroer, W.F., Amin, S.A., Bates, N.R., Bertrand, E.M., et al., 2022b. Microbial metabolites in the marine carbon cycle. Nat. Microbiol. 7, 508–523. https://doi.org/10.1038/s41564-022-01090-3.

Murillo, A.A., Ramírez-Flandes, S., DeLong, E.F., Ulloa, O., 2014. Enhanced metabolic versatility of planktonic sulfur-oxidizing γ-proteobacteria in an oxygen-deficient coastal ecosystem. Front. Mar. Sci. 1, 10.3389/fmars.2014.00018.
Nelson, D.M., Treguer, P., Brzezinski, M.A., Leynaert, A., Queguiner, B., 1995. Production and dissolution of biogenic silica in the ocean - revised global estimates, comparison with regional data and relationship to biogenic sedimentation. Glob. Biogeochem. Cycles 9, 359–372. https://doi.org/10.1029/95gb01070.
Nguyen, R.T., Harvey, H.R., 1997. Protein and amino acid cycling during phytoplankton decomposition in oxic and anoxic waters. Org. Geochem. 27, 115–128. https://doi.org/10.1016/S0146-6380(97)00076-4.
Pantoja, S., Sepúlveda, J.S., González, H.E., 2004. Decomposition of sinking proteinaceous material during fall in the oxygen minimum zone off northern Chile. Deep-Sea Research Part I-Oceanographic Research Papers 51, 55–70. https://doi.org/10.1016/j.dsr.2003.09.005.
Pantoja, S., Rossel, P., Castro, R., Cuevas, L.A., Daneri, G., Córdova, C., 2009. Microbial degradation rates of small peptides and amino acids in the oxygen minimum zone of Chilean coastal waters. Deep-Sea Research Part Ii-Topical Studies in Oceanography 56, 1019–1026. https://doi.org/10.1016/j.dsr2.2008.09.007.
Ploug, H., Kuhl, M., BuchholzCleven, B., Jorgensen, B.B., 1997. Anoxic aggregates - an ephemeral phenomenon in the pelagic environment? Aquat. Microb. Ecol. 13, 285–294. https://doi.org/10.3354/ame013285.
Pohlabeln, A.M., Gomez-Saez, G.V., Noriega-Ortega, B.E., Dittmar, T., 2017. Experimental evidence for abiotic sulfurization of marine dissolved organic matter. Front. Mar. Sci. 4, 364. https://doi.org/10.3389/fmars.2017.00364.
Pucher, M., Wünsch, U., Weigelhofer, G., Murphy, K., Hein, T., Graeber, D., 2019. staRdom: versatile software for analyzing spectroscopic data of dissolved organic matter in R. Water 11. https://doi.org/10.3390/w11112366.
Ragavan, P., Kumar, S., 2021. Potential role of priming effect in the open ocean oxygen minimum zones: an outlook. Hydrobiologia 848, 2437–2448. https://doi.org/10.1007/s10750-021-04574-1.
Raven, M.R., Keil, R.G., Webb, S.M., 2021a. Microbial sulfate reduction and organic sulfur formation in sinking marine particles. Science 371, abc6035. https://doi.org/10.1126/science.abc6035.
Raven, M.R., Keil, R.G., Webb, S.M., 2021b. Rapid, concurrent formation of organic sulfur and iron sulfides during experimental sulfurization of sinking marine particles. Glob. Biogeochem. Cycles 35, e2021GB007062. https://doi.org/10.1029/2021GB007062.
Sinu, J.V., 2022. Source and composition of organic matter and its role in designing sediment microbial communities. In: Prince, S., Godson, S.G.T.V., Krishnakumar, S. (Eds.), Microbial Communities in Coastal Sediments: Structure and Functions. Elsevier, pp. 83–133.
Spietz, R.L., Williams, C.M., Rocap, G., Horner-Devine, M.C., 2015. A dissolved oxygen threshold for shifts in bacterial community structure in a seasonally hypoxic estuary. PLoS One 10. https://doi.org/10.1371/journal.pone.0135731.
Teeling, H., Fuchs, B.M., Bennke, C.M., Krüger, K., Chafee, M., Kappelmann, L., et al., 2016. Recurring patterns in bacterioplankton dynamics during coastal spring algae blooms. Elife 5. https://doi.org/10.7554/eLife.11888.
Vandewiele, S., Cowie, G., Soetaert, K., Middelburg, J.J., 2009. Amino acid biogeochemistry and organic matter degradation state across the Pakistan margin oxygen minimum zone. Deep-Sea Research Part Ii-Topical Studies in Oceanography 56, 376–392. https://doi.org/10.1016/j.dsr2.2008.05.035.
Wang, B., Chen, J.F., Jin, H.Y., Li, H.L., Huang, D.J., Cai, W.J., 2017. Diatom bloom-derived bottom water hypoxia off the Changjiang estuary, with and without typhoon influence. Limnol. Oceanogr. 62, 1552–1569. https://doi.org/10.1002/lno.10517.
Wang, H.J., Dai, M.H., Liu, J.W., Kao, S.J., Zhang, C., Cai, W.J., et al., 2016. Eutrophication-driven hypoxia in the East China Sea off the Changjiang estuary. Environ. Sci. Technol. 50, 2255–2263. https://doi.org/10.1021/acs.est.5b06211.
Wang, X., Xia, K., Yang, X.J., Tang, C., 2019. Growth strategy of microbes on mixed carbon sources. Nat. Commun. 10. https://doi.org/10.1038/s41467-019-09261-3.
Wang, X.L., Wang, M.X., Xie, X.G., Guo, S.Y., Zhou, Y., Zhang, X.B., et al., 2020. An amplification-selection model for quantified rhizosphere microbiota assembly. Sci. Bull. 65, 983–986. https://doi.org/10.1016/j.scib.2020.03.005.
Wang, Z.H., Ge, Y.F., Bi, S.S., Liang, Y.M., Shi, Q., 2022. Molecular characterization of organic aerosol in winter from Beijing using UHPLC-Orbitrap MS. Sci. Total Environ. 812. https://doi.org/10.1016/j.scitotenv.2021.151507.
West, N.J., Obernosterer, I., Zemb, O., Lebaron, P., 2008. Major differences of bacterial diversity and activity inside and outside of a natural iron-fertilized phytoplankton bloom in the Southern Ocean. Environ. Microbiol. 10, 738–756. https://doi.org/10.1111/j.1462-2920.2007.01497.x.
Williams, T.J., Wilkins, D., Long, E., Evans, F., DeMaere, M.Z., Raftery, M.J., et al., 2013. The role of planktonic in processing algal organic matter in coastal East Antarctica revealed using metagenomics and metaproteomics. Environ. Microbiol. 15, 1302–1317. https://doi.org/10.1111/1462-2920.12017.
Wright, J.J., Konwar, K.M., Hallam, S.J., 2012. Microbial ecology of expanding oxygen minimum zones. Nat. Rev. Microbiol. 10, 381–394. https://doi.org/10.1038/nrmicro2778.
Wu, C.H., Yang, J., Fu, Q., Zhu, B., Ruan, T., Jiang, G.B., 2019. Molecular characterization of water-soluble organic compounds in PM2.5 using ultrahigh resolution mass spectrometry. Sci. Total Environ. 668, 917–924. https://doi.org/10.1016/j.scitotenv.2019.03.031.
Xiao, S.C., Chen, J.X., Shen, Y., Chen, Q., Wang, Y., Li, Y.Y., et al., 2023. Molecular characterization of organic matter transformation mediated by microorganisms under anoxic/hypoxic conditions. Science China-Earth Sciences 66, 894–909. https://doi.org/10.1007/s11430-022-1080-8.
Yamashita, Y., Tanoue, E., 2008. Production of bio-refractory fluorescent dissolved organic matter in the ocean interior. Nat. Geosci. 1, 579–582. https://doi.org/10.1038/ngeo279.
Yamashita, Y., Cory, R.M., Nishioka, J., Kuma, K., Tanoue, E., Jaffé, R., 2010. Fluorescence characteristics of dissolved organic matter in the deep waters of the Okhotsk Sea and the northwestern North Pacific Ocean. Deep-Sea Research Part Ii-Topical Studies in Oceanography 57, 1478–1485. https://doi.org/10.1016/j.dsr2.2010.02.016.
Yamuza-Magdaleno, A., Jiménez-Ramos, R., Casal-Porras, I., Brun, F.G., Egea, L.G., 2024. Long-term sediment organic carbon remineralization in different seagrass and macroalgae habitats: implication for blue carbon storage. Front. Mar. Sci. 11. https://doi.org/10.3389/fmars.2024.1370768.
Ye, Q., Wu, Y., Zhu, Z.Y., Wang, X.N., Li, Z.Q., Zhang, J., 2016. Bacterial diversity in the surface sediments of the hypoxic zone near the Changjiang estuary and in the East China Sea. Microbiologyopen 5, 323–339. https://doi.org/10.1002/mbo3.330.
Yu, T.T., Wu, W.C., Liang, W.Y., Wang, Y.Z., Hou, J.L., Chen, Y.R., et al., 2023. Anaerobic degradation of organic carbon supports uncultured microbial populations in estuarine sediments. Microbiome 11. https://doi.org/10.1186/s40168-023-01531-z.
Zakem, E.J., Follows, M.J., 2017. A theoretical basis for a nanomolar critical oxygen concentration. Limnol. Oceanogr. 62, 795–805. https://doi.org/10.1002/lno.10461.
Zhang, X.D., Wang, Z.L., Cai, H.W., Chai, X.P., Tang, J.L., Zhuo, L.F., et al., 2022. Summertime dissolved oxygen concentration and hypoxia in the Zhejiang coastal area. Front. Mar. Sci. 9. https://doi.org/10.3389/fmars.2022.1051549.
Zhao, L.Y., Qin, H.W., Zhang, M.L., Xin, R.Y., Liu, J.C., Wang, M.J., et al., 2025a. Effect of marine anoxia on the conversion of macroalgal biomass to refractory dissolved organic carbon. Mar. Environ. Res. 204. https://doi.org/10.1016/j.marenvres.2025.106956.
Zhao, L.Y., Xing, H.Y., Xin, R.Y., Liu, J.C., Qin, H.W., Ma, Y.Q., et al., 2025b. Marine anoxia impede the transformation of dissolved organic carbon released by kelp into refractory dissolved organic carbon. Mar. Pollut. Bull. 211. https://doi.org/10.1016/j.marpolbul.2024.117429.
Zhao, Z., Gonsior, M., Schmitt-Kopplin, P., Zhan, Y.C., Zhang, R., Jiao, N.Z., et al., 2019. Microbial transformation of virus-induced dissolved organic matter from picocyanobacteria: coupling of bacterial diversity and DOM chemodiversity. ISME J. 13, 2551–2565. https://doi.org/10.1038/s41396-019-0449-1.
Zheng, Q., Wang, Y., Lu, J., Lin, W., Chen, F., Jiao, N., 2020. Metagenomic and metaproteomic insights into photoautotrophic and heterotrophic interactions in a *Synechococcus* culture. mBio 11, 10.1128/mBio.03261-19.
Zheng, Q., Lin, W., Wang, Y., Li, Y., He, C., Shen, Y., et al., 2021. Highly enriched N-containing organic molecules of *Synechococcus* lysates and their rapid transformation by heterotrophic bacteria. Limnol. Oceanogr. 66, 335–348. https://doi.org/10.1002/lno.11608.
Zhou, F., Chai, F., Huang, D.J., Wells, M., Ma, X., Meng, Q.C., et al., 2020. Coupling and decoupling of high biomass phytoplankton production and hypoxia in a highly dynamic coastal system: the Changjiang (Yangtze River) estuary. Front. Mar. Sci. 7, 10.3389/fmars.2020.00259.
Zhou, J., Zhu, Z.Y., Hu, H.T., Zhang, G.L., Wang, Q.Q., 2021. Clarifying water column respiration and sedimentary oxygen respiration under oxygen depletion off the Changjiang estuary and adjacent East China Sea. Front. Mar. Sci. 7, 623581. https://doi.org/10.3389/fmars.2020.623581.
Zhu, Z.Y., Zhang, J., Wu, Y., Zhang, Y.Y., Lin, J., Liu, S.M., 2011. Hypoxia off the Changjiang (Yangtze River) estuary: oxygen depletion and organic matter decomposition. Mar. Chem. 125, 108–116. https://doi.org/10.1016/j.marchem.2011.03.005.
Zhu, Z.Y., Wu, H., Liu, S.M., Wu, Y., Huang, D.J., Zhang, J., et al., 2017. Hypoxia off the Changjiang (Yangtze River) estuary and in the adjacent East China Sea: quantitative approaches to estimating the tidal impact and nutrient regeneration. Mar. Pollut. Bull. 125, 103–114. https://doi.org/10.1016/j.marpolbul.2017.07.029.